



## **Antibacterial Activities of Calcareous/TiO<sub>2</sub> Nanocomposites**

**P. Mariselvi<sup>1</sup> and T. Anantha Kumar<sup>2\*</sup>**

<sup>1</sup>PG and Research Department of Chemistry, Rani Anna Govt. College for Women, Tirunelveli, Affiliated to Manonmaniam Sundaranar University, Tirunelveli – 627 012, Tamilnadu, India.

<sup>2</sup>Department of Chemistry, Merit Arts and Science College, Idaikal, Affiliated to Manonmaniam Sundaranar University, Tirunelveli – 627 012, Tamilnadu, India.

### **Authors' contributions**

This work was carried out in collaboration between both authors. Both authors read and approved the final manuscript.

### **Article Information**

DOI: 10.9734/JPRI/2021/v33i42B32455

#### **Editor(s):**

(1) Dr. Asmaa Fathi Moustafa Hamouda, Jazan University, Saudi Arabia.

#### **Reviewers:**

(1) Emad Mahmoud Ibrahim Elsehly, Damanhour University, Egypt.

(2) Divya. R, S.T. Hindu College, M.S. University, India.

Complete Peer review History: <https://www.sdiarticle4.com/review-history/72834>

**Original Research Article**

**Received 22 June 2021**  
**Accepted 29 August 2021**  
**Published 03 September 2021**

### **ABSTRACT**

**Aims:** In the present investigation, To synthesis, characterization and antibacterial activity of Calcareous/TiO<sub>2</sub> nanocomposites toward *Bacillus*, *Proteus vulgaris*, *Micrococcus luteus*, *Staphylococcus aureus* and *Escherichia coli*.

**Methodology:** The resulting Calcareous/TiO<sub>2</sub> nanocomposite was synthesized by hydrothermal method. The synthesized nanocomposites were characterized by using XRD, SEM with EDAX, AFM, TEM and UV-Vis absorption spectroscopy. The antibacterial activities of the Calcareous/TiO<sub>2</sub> nanocomposite species were checked by using agar well diffusion method.

**Results:** The XRD pattern is showed that the diffraction peaks appear in the pattern corresponding to the anatase phase of TiO<sub>2</sub>. UV-Visible spectrum showed that the blue shifted when compared with bulk TiO<sub>2</sub> (3.2 eV). The blue shift might be caused by nanosize effect and structural defect of nanomaterials. AFM image shows the morphology of Calcareous/TiO<sub>2</sub> nanocomposites forming sharp particles on the surface. TEM image showed that the particles exhibit a relatively uniform particle size distribution. The average size of the nanocomposites estimated from the TEM image is around 50nm.

**Conclusion:** In conclusion, the Calcareous/TiO<sub>2</sub> nanocomposites have been successfully synthesized. The prepared nanocomposites were characterized using various analytical tools like XRD, SEM with EDAX, AFM, TEM, UV-Vis absorption spectrum.

**Keywords:** Antibacterial activity; calcareous; nanocomposites; bacillus; e.coli; nanotechnology.

## 1. INTRODUCTION

In the last few years, nanotechnology had been flourishing. The improvement of Nano materials is a basis for the development of nanoscience and nanotechnology. Nano materials consult with special properties, whose geometric dimension reaches Nano scale. Among Nanomaterials, brilliant significance has been connected to Nano oxide [1-3]. Nano-structured materials are attracting a brilliant deal of interest due to their ability for accomplishing particular tactics and selectivity, in particular in organic and pharmaceutical applications [4-6]. Nano-Materials are referred to as a wonder of modern medicine. It's said that antibiotics kill possibly a half dozen different diseases-causing organisms but Nano-materials can kill some 650 cell [7]. Resistant strains fail to broaden if we observe Nanoparticle-primarily based totally formulations of their media. In laboratory assessments with Nanoparticles, the micro organism, viruses, and fungi are killed inside mins of contact. The impact of nanoparticles on micro organism could be very important, since they represent the lowest level and hence enter the food chain of ecosystem [8]. In recent years, various nanoparticles have been reported to display good biological activities [9]. Amongst them, TiO<sub>2</sub> nanoparticles have attracted the attention of researchers due to its oxidative and hydrolysis properties. As a photocatalyst, it can improve the efficiency of electrolytically splitting water into hydrogen and oxygen which can produce electricity in nanoparticles form. When these nanoparticles are exposed to ultraviolet (UV) light, they become increasingly hydrophilic [10]. In the case of antibacterial coatings, maximum density of nonmaterial on surface results in the generation of reactive oxygen species (ROS) and thus increases the antibacterial activity of TiO<sub>2</sub> [11]. TiO<sub>2</sub> photocatalysts have also been utilized to disinfect a broad spectrum of microorganisms [12]. Recently the metal oxide nanoparticles played a vital role in the novel drug delivery systems. Recent studies have demonstrated that specially formulated metal oxide nanoparticles have good antibacterial activity [13] and antimicrobial formulations comprising nanoparticles could be effective bactericidal

materials [14-15]. TiO<sub>2</sub> nanoparticles (TiO<sub>2</sub>-NPs), approximately less than 100 nm in diameter, have become a new generation of advanced materials because of their novel and fascinating optical, dielectric, and photo-catalytic properties from size quantization [16].

Antimicrobial activity of TiO<sub>2</sub> was observed in 1985 by Mat-sunaga and colleagues, who stated that microbial cells might be killed by the contact with a TiO<sub>2</sub>-Pt catalyst under illumination with near UV light [17]. Since then, many researchers have investigated the disinfection capability of photocatalysis the use of TiO<sub>2</sub>, each powder and film, as photocatalysts [17-20]. According to literature data, distinctly reactive oxygen species (ROS) are concept to be the key species in the photocatalytic disinfection process. In fact, the photo-generated holes and electrons trapped on the surface of the semiconductor react with adsorbed species to initiate the formation of distinctly reactive oxygen species (ROS), •OH, O<sub>2</sub>•- and H<sub>2</sub>O<sub>2</sub>•, able to mineralizing pollutants. All three ROS exhibit bactericidal activity but some studies have emphasized that the hydroxyl radical should be the most important oxidant species responsible for the attack of the bacterial cell wall, leading to modifications of membrane permeability and cell death [18-20]. Bindu Arora et al., investigated, an exposure of UV irradiation of 60 minutes has shown to greatly enhance the antibacterial efficacy of TiO<sub>2</sub> nanoparticle against MDR *P. aeruginosa*. Further, the antibiotic CEF potency was increased when used in combination with 60 minutes UV-irradiated TiO<sub>2</sub> nanoparticles. This synergistic study against the pathogens offers its application potential in clinical diagnostics as an attempt to find a solution to the growing problem of antibiotic resistance [21]. The antibacterial activity of Clay-TiO<sub>2</sub> nanocomposite, there are four types of bacteria *Micrococcus*, *Staphylococcus aureus* as a Gram-positive bacterium, and *E. coli* and *Pseudomonas aeruginosa* as a Gram-negative bacterium, were used as model bacteria in this study. Our results showed good inhibition on two types of bacteria, *E. coli* and *Micrococcus*, even under room light by Lashgari et al., [22]. Alireza et al., [23] reported the Antibacterial treatment of Ag/TiO<sub>2</sub> nanocomposites was able to reduce

bacterial growth by approximately 75%. This result indicated that the bacteria were successfully eradicated with Ag/TiO<sub>2</sub> nanocomposites. In general, the effect of adding Ag/TiO<sub>2</sub> will give more significant effect on the performance of nanocomposite materials to eradicate *S. aureus*. The result is strongly dependent on the growth temperature and baking time to produce and increase the amount of nanorods that have been proven more effective to eradicate bacteria. According to the work of Sahar *et al.*, [24] functionalized MWNTs investigated antimicrobial activities against both gram-negative (*E. coli*) and gram-positive (*S. aureus*) bacteria. In fact, F-MWNTs showed the best antibacterial activities compared to commercial antibiotics. The results demonstrate that the best concentration of F-MWNTs for the utmost inhibition and antibacterial functionality is 80 and 60 µg/ml for *E. coli* and *S. aureus*, respectively.

Popov *et al.*, [25] investigated the relationship between the structural properties of materials based on multi-walled carbon nanotubes and therefore the vital activity of bacteria *E. Coli* strain M-17. They have different wettability, and as a result they have different effects on bacterial cells. Samples with the highest hydrophilicity showed the least bacterial biocompatibility.

The benefits of the usage of those inorganic oxide nanocomposites as antimicrobial agents are their more effectiveness on resistant strains of microbial pathogens, much less toxicity and warmth resistance [26-27]. Also, they provide mineral components essential to human cells and even small amounts of them show strong activity [28-29]. These metallic oxide nanocomposites have many significant features such as chemical and physical stability, antibacterial activity, intensive ultraviolet and infrared adsorption with a broad range of applications as semiconductors, sensors, transparent electrodes, solar cells, etc [30]. The present investigation was aimed to production a new nanocomposites of TiO<sub>2</sub> and determination of antibacterial activity of this nanocomposites toward *Bacillus*, *P. Vulgaris*, *M. Luteus*, *S. Aureus* and *E. coli*. In our previous paper was reported the synthesis, characterization and photocatalytic activity of Calcareous/TiO<sub>2</sub> nanocomposites [31].

## 2. MATERIALS AND METHODS

### 2.1 Experimental Method

Calcareous – water dispersion (1% w/w) was stirred for 2 hours. An aliquot of TiO<sub>2</sub> sol was added to the dispersion, to obtain a final TiO<sub>2</sub> content of 70% w/w. The slurry was stirred for 24 hours. The resulting dispersion was centrifuged at 3800 rpm for 10 minutes. The solid phase was washed with ultrapure water followed by triplicate centrifugation. The resulting Calcareous – TiO<sub>2</sub> composite was dispersed in 1:1 water: ethanol solution, prior to hydrothermal treatment in an autoclave at 180 °C for 5 hours. The product was centrifuged once again at 3800 rpm for 15 minutes, and oven dried at 60 °C for 3 hours [31].

### 2.2 Instrumental Characterizations

XRD measurements are performed using a Philips diffractometer of 'X' pert company with monochromatized Cu K $\alpha$  ( $\lambda=1.54060$  Å) radiation. For determination of crystallite size, Debye Scherrer's analysis on XRD is commonly used. A double beam UV-Vis (Jascow – 500) spectrophotometer with 1 mm optical path length quartz cells was used for all absorbance measurement in the range of 200 nm – 800 nm. SEM image was obtained by using HITACHI-S-3400H model. TEM image was obtained by using Jeol/JEM 2100. Atomic Force Microscopy (AFM; VeecoCP-II) in contact mode using Si tips at a scan rate of 1 Hz.

### 2.3 Agar Well Diffusion Assay

The antibacterial activities of the Calcareous/TiO<sub>2</sub> nanocomposite species were checked by using agar well diffusion method [32]. The antibacterial activity against *Bacillus*, *P. vulgaris*, *M. luteus*, *S. aureus* and *E. coli*. The nanocomposites were dissolved in some polar solvents like ethanol, methanol etc. Mueller Hinton agar was prepared, sterilized and poured into petri plates. The test organisms were spread on these plates on which wells were made using a sterile corkborer. To each well, 30 µl of each nanocomposites are added and plates were incubated at 30°C for 24 hrs. After incubation, the results were recorded by measuring the diameter of zone of inhibition surrounding the well.

### 3. RESULTS AND DISCUSSION

#### 3.1 XRD Analysis of Calcareous /TiO<sub>2</sub> Nanocomposites

The X-ray diffraction analysis is used to determine the particle size and to study the structural properties of the synthesized nanocomposites of TiO<sub>2</sub>, the powder XRD analysis was performed, which is shown in Fig.1. It could be clearly observed that the diffraction peaks appear in the pattern corresponding to the anatase phase of TiO<sub>2</sub>. The spectra showed crystalline nature with 2θ peaks lying at 2θ=25.25° (101), 2θ=37.8° (004), 2θ=47.9° (200), 2θ =53.59° (105) and the average crystallite size has been calculated from the recorded XRD patterns using well known Debye Scherrer equation  $D=0.89\lambda/\beta\cos\theta$  of Calcareous/TiO<sub>2</sub> nanocomposites has been found to be 16 nm respectively. The similar result was reported by Daimei Chen *et al.* [33].

#### 3.2 SEM with EDAX Analysis of Calcareous /TiO<sub>2</sub> Nanocomposites

Scanning electron microscope (SEM) was used for the morphological study of Calcareous/TiO<sub>2</sub> nanocomposites. Fig.2.a. suggests the SEM images of the as prepared metallic oxide nanocomposites. The Calcareous/TiO<sub>2</sub> nanocomposites formed had been highly agglomerated. The spherical shaped particles with clumped distributions are seen via the SEM analysis. The result was properly matched with Suresh *et al.*[34]. The elemental presences are given in fig.2.b. The surface of synthesized nanoparticles was characterized the use of FESEM. The micrograph confirmed nano-scaled TiO<sub>2</sub> particles with the detailed surface morphology of nanoparticles (NPs) and microspheres. The nanoparticles are poorly dispersed with spherical clusters with agglomeration size up to 95 nm. Agglomeration makes it tough to study individual nanoparticles. This result was also reported by Rajakumar *et al.*[35] and Karen *et al* [36].

#### 3.3 AFM Analysis of Calcareous /TiO<sub>2</sub> Nanocomposites

Atomic force microscopic (AFM) is used to get microscopic information on the surface structure and to plot topographies representing the surface relief. This technique offers digital images, which permit quantitative measurements of surface

features, such as root mean square roughness, Rq, or average roughness Ra, and the analysis of images from different perspectives, including three-dimensional simulation [37]. It may be seen, the morphology of Calcareous/TiO<sub>2</sub> nanocomposites forming sharp particles on the surface in Figure.3.a. and 3.b. While Fig. 3.a. suggests the AFM 2D surface morphology of nanocomposite with rounded particles on the surface. The particles are not clearly visible and not fully homogenous. This result was reported by Nur *et al* [38] and Saja *et al* [39] that is, the AFM image showed high uniform distribution of particles with spherical shape. The statistical roughness evaluation confirmed that the obtained roughness average is 0.422 nm, root mean square roughness is 0.513nm, surface skewness is - 0.0806, and the surface kurtosis is identical to 2.47. The AFM results show that the surface of TiO<sub>2</sub> is bumpy and the valleys are more than the peaks of surface [40].

#### 3.4 TEM Analysis of Calcareous/TiO<sub>2</sub> Nanocomposites

The transmission electron spectroscopic analysis was executed to verify the actual size of the particles, their growth pattern and the distribution of the crystallites. Fig.4 suggested a typical TEM image of the Calcareous/TiO<sub>2</sub> nanocomposites. It may be seen that the particles exhibit a relatively uniform particle size distribution. The average size of the Calcareous/TiO<sub>2</sub> nanocomposites predicted from the TEM image is around 50nm.

#### 3.5 UV-vis Absorption Spectroscopy

The UV visible spectrum observed that the absorption edge shifted towards lower wavelength for Calcareous/TiO<sub>2</sub> nanocomposites is given in figure.5.a. This is clearly indicated an increase in the band gap energy of Calcareous/TiO<sub>2</sub> nanocomposites. The band gap energy can be estimated from the following equation.

$$\alpha = \frac{k(h\nu - E_g)^{n/2}}{h\nu}$$

Plots of  $(\alpha h\nu)^2$  versus photon energy (hν) for Calcareous/TiO<sub>2</sub> nanocomposites is given in figure.5.b. (using Tauc plot). The band gap energy is evaluated from the intercept of the tangents of the plot is 3.5 eV. This revealed that the blue shifted when compared with the bulk TiO<sub>2</sub> (3.2 eV). The blue shift might be caused by nanosize effect and structural defect of nanomaterials [31].

### 3.6 Antibacterial Activity on Calcareous/TiO<sub>2</sub> Nanocomposites

Fresh cultures (24 h) of *Bacillus*, *P. vulgaris*, *M. luteus*, *S. aureus* and *E. coli* were diluted in saline. A sterile swab was dipped within the diluted cultures and spread over the agar. Wells were made in the inoculated agar medium, employing a sterile borer (6 mm in diameter) and 30  $\mu$ L of the nanocomposite supernatants were pipette into the wells. The agar plates were incubated at 30°C for twenty four hours, after which zones of inhibitions were observed and antibacterial activity was measured in terms of zone of inhibition (mm). Antimicrobial activity of the antibiotic showed a clear inhibition zone within the media seeded with *Bacillus* (26 mm), *P. vulgaris* (35 mm), *M. luteus* (28 mm), *S. aureus* (32 mm) and *E.coli* (30 mm). Zone of inhibition against bacterial strain by calcareous/TiO<sub>2</sub> nanocomposite given in Table.1. The bactericide activity of Calcareous/TiO<sub>2</sub> nanocomposites was evaluated in absence of light, through detection of lowest concentration of Calcareous/TiO<sub>2</sub> nanocomposites where no growth is visually observed for Gram-negative bacteria *E.coli* and Gram-positive bacteria *S. aureus*. Only the Calcareous/TiO<sub>2</sub>

nanocomposites exhibited biocide effect at nanocomposites contents greater. Thus hydroxyl groups or oxygen vacancies (O<sup>-</sup>) on TiO<sub>2</sub> surface haven't enough antibacterial power. This result was reported by Zoe *et al* [41]. During this case, Ag NPs supported on TiO<sub>2</sub> can certainly increase the antibacterial performance more effectively than TiO<sub>2</sub> by itself. We obtained an adequate attachment of a high Ag NPs number on the TiO<sub>2</sub> surface, with a homogeneous dispersion and high available superficial area in strong alkaline suspension of TiO<sub>2</sub>.

Many studies issue the ability of using of metal oxide nanoparticles as alternative solution to antibiotics due to strong germicidal nature of it. In this experiment the strain of *E.coli* and *S. aureus* were inoculated in Muller Hinton medium with different concentrations of TiO<sub>2</sub> nanoparticles. The MIC value of TiO<sub>2</sub> nanoparticles was 30  $\mu$ g/mL, for *E.coli* and 40 $\mu$ g/ml for *S. aureus*. Basically the growth of *E.coli* and *S. aureus* inhibited compared to the control and the results inversely proportional with increasing the concentration of TiO<sub>2</sub> nanoparticles, these results assured with the agar diffusion methods which show remarked susceptibilities of *E.coli* and *S. aureus* to TiO<sub>2</sub> nanoparticles from the results.

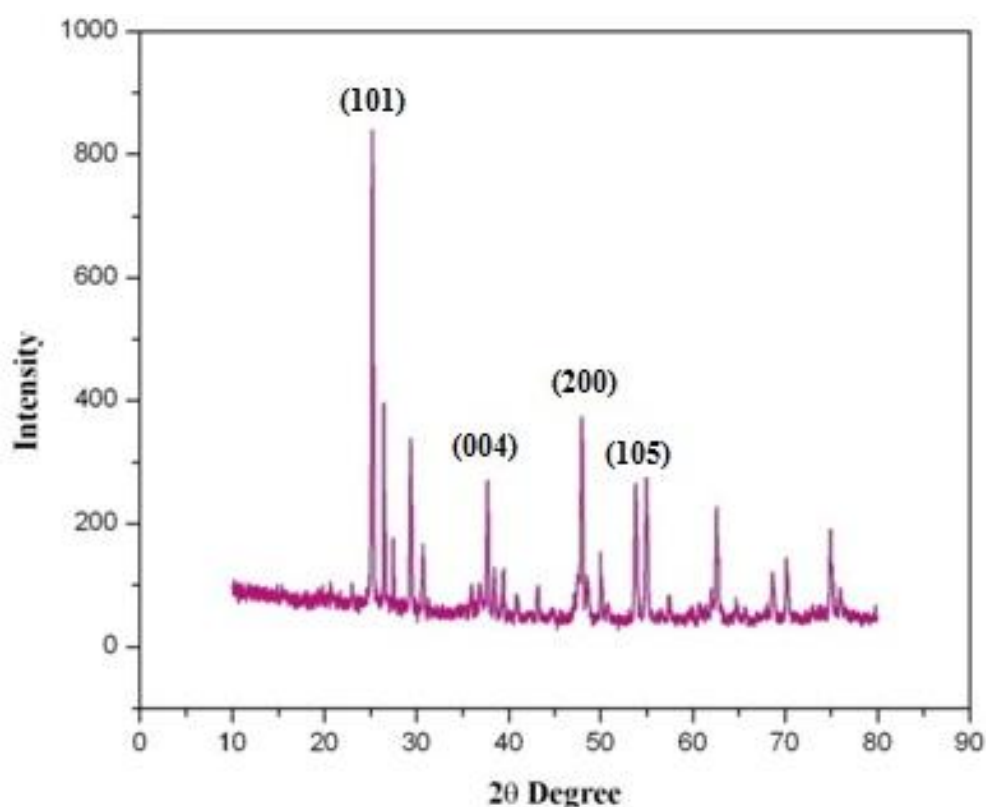


Fig. 1. XRD pattern of calcareous/TiO<sub>2</sub> nanocomposites

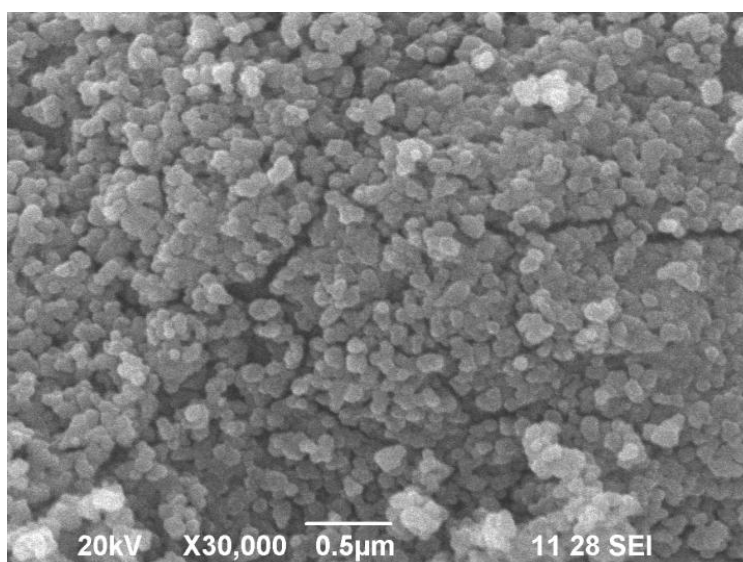


Fig. 2a. SEM image of calcareous/TiO<sub>2</sub> nanocomposites

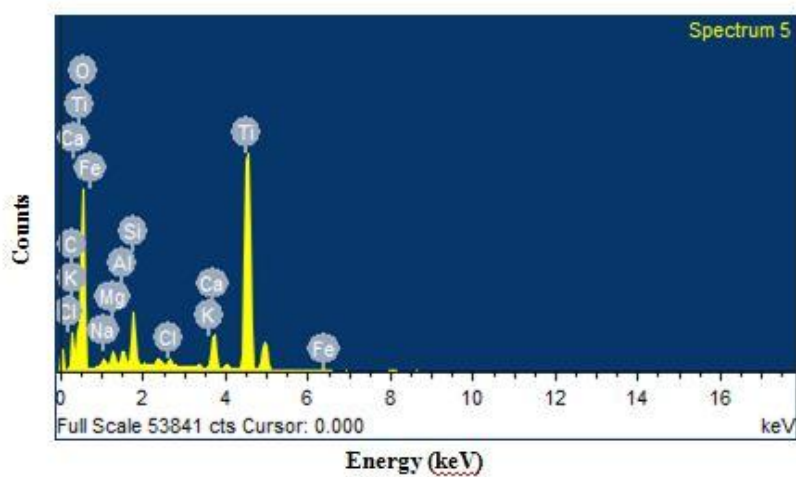


Fig. 2b. EDAX spectrum of calcareous/TiO<sub>2</sub> nanocomposites

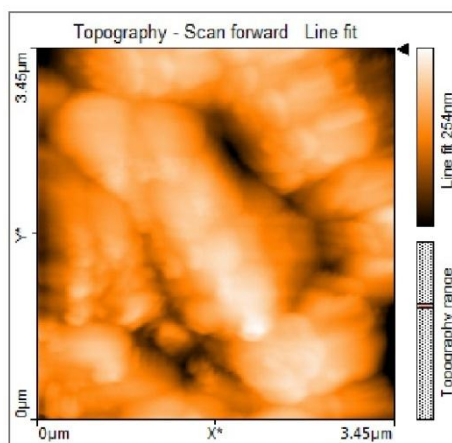


Fig. 3.a. AFM 2D image of calcareous/TiO<sub>2</sub> nanocomposites

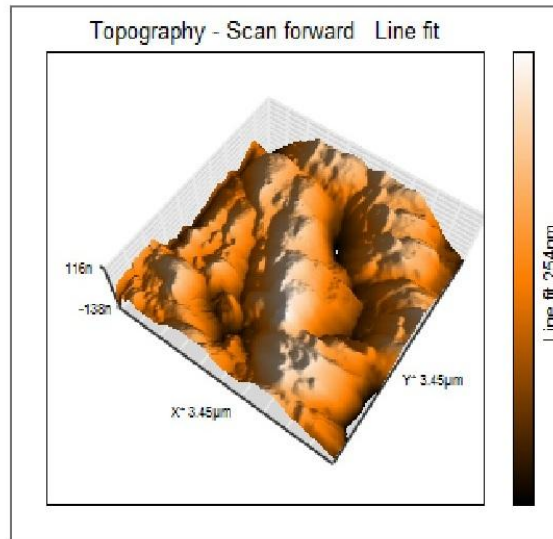


Fig. 3.b. AFM 3D image of calcareous/TiO<sub>2</sub> nanocomposites

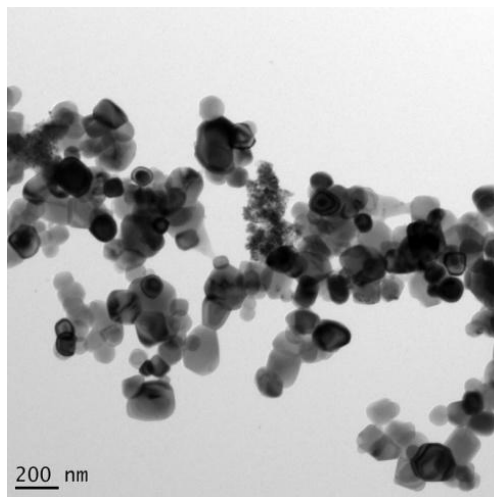


Fig.4. TEM image of calcareous/TiO<sub>2</sub> nanocomposites

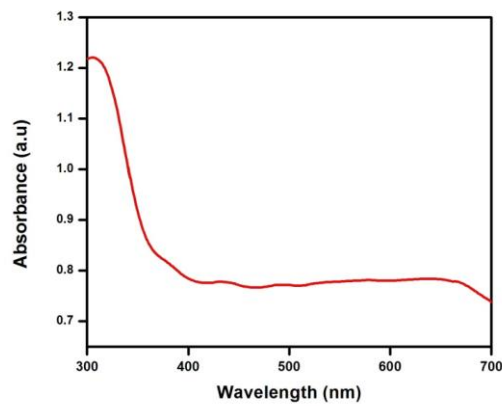


Fig. 5.a. UV-vis absorption spectrum of calcareous/TiO<sub>2</sub> nanocomposites



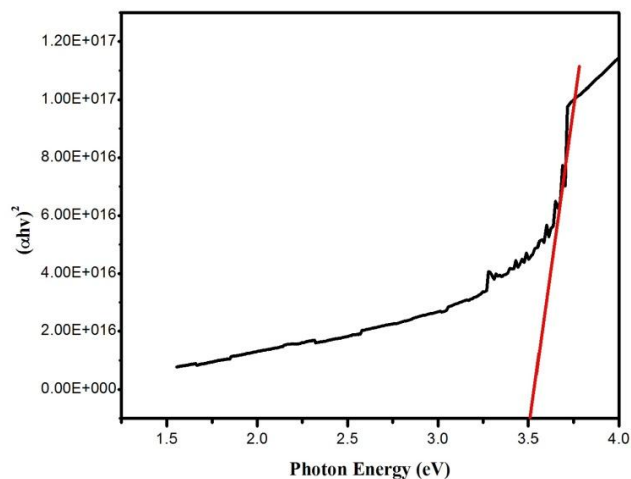


Fig. 5.b. Band gap energy of calcareous/TiO<sub>2</sub> nanocomposites

Table 1. Zone of inhibition against strains by Calcareous/TiO<sub>2</sub> Nanocomposites

Nanocomposites	<u>Zone of inhibition (in mm)</u>				
	<i>Bacillus</i>	<i>Proteus vulgaris</i>	<i>Micrococcus luteus</i>	<i>Staphylococcus aureus</i>	<i>E. coli</i>
Calcareous/TiO <sub>2</sub>	26	35	28	32	30



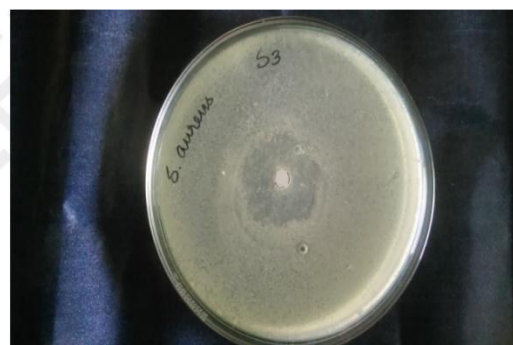
6.a. *Bacillus*



6.b. *P. vulgaris*



6.c. *M.luteus*



6.d. *S. aureus*



6.e. *E. coli***Fig. 6. Antibacterial activities of calcareous/TiO<sub>2</sub> nanocomposites**

Several studies have believed the germicidal mechanisms of TiO<sub>2</sub> nanoparticles involving release of positively charge ions to reaction medium linked to (negative charges) thiol group (-SH) of the proteins on the cytoplasmic membrane reported by Jayaseelan *et al* [42]. This reaction lead to capture the cell wall and increased permeability beside it causes deform the structure of cellular components such as DNA, ribosomes and cellular enzymes and finally death of microbial cell by Koseki *et. al* [43]. The antibacterial activity figures are given in 6.a, 6.b, 6.c, 6.d, 6.e. In our previous report, Antibacterial activity of Illite/TiO<sub>2</sub> nanocomposites showed that the zone inhibition was found against *E.coli* (15mm), *S. aureus* (18mm) and *Bacillus* (13mm) with respect to the control ampicillin [44]. Mariselvi *et al.*, [45] investigated the antibacterial activity of Kaolinite/TiO<sub>2</sub> nanocomposites, which is a clear inhibition zone in the media seeded with *S.aureus* (19mm), *M.luteus* (20 mm) and *E.coli* (24 mm). According to the Pohan and co-workers [46] carried out the antibacterial properties of [Ag TiO<sub>2</sub>]:Clay nanocomposites. They studied antibacterial activity in dark and activity under visible light irradiation. The AgTiO<sub>2</sub>:Clay nanocomposites displays good antibacterial activity for *S.aureus* without and under visible light exposure. The diameter of inhibition zone increases from 2 to 8 mm in the dark and 8 to 12 mm under light irradiation. For *E.coli*, we observed, significant antibacterial activity only under visible light irradiation due to the cell wall layers of this bacterium. In other case, antibacterial activity of TiO<sub>2</sub>, GNSAC, TiO<sub>2</sub>/GNSAC nanoparticles were tested against gram positive bacteria *V. cholerae*. The TiO<sub>2</sub>/GNSAC (7 mm) nanoparticles show maximum zone inhibition than GNSAC (4 mm) and TiO<sub>2</sub> (5 mm) nanoparticles [47]. Alireza *et*

*al.*, [48] demonstrated the antibacterial activity of NiFeO<sub>4</sub>/PAMA/Ag-TiO<sub>2</sub> nanocomposites showed zone of inhibition was found against *S.aureus* (21mm), *B.cereus* (18mm), *E.coli* (18.5 mm) and *S.typhimurium* (22mm). This nanocomposites has greater antibacterial activity. In our case, antibacterial activity of calcareous/TiO<sub>2</sub> nanocomposites has greater antibacterial activity than above reports.

#### 4. CONCLUSION

In summary the Calcareous/TiO<sub>2</sub> nanocomposites have been successfully synthesized. The prepared nanocomposites were characterized using various analytical tools like XRD, SEM with EDAX, AFM, TEM, UV-Vis absorption spectrum. The X-ray diffraction result revealed that the presence of anatase phase of TiO<sub>2</sub>. The synthesized nanocomposites size and morphology of the sample were characterized by SEM with EDAX. SEM proved the spherical shape and well dispersed on the clay surface. AFM analysis shows the morphology of Calcareous/TiO<sub>2</sub> Nanocomposites forming sharp particles on the surface and while the AFM 2D surface morphology of nanocomposite with rounded particles on the surface. TEM analysis indicated that the particles exhibit a relatively uniform particle size distribution. The band gap energy of this nanocomposite is 3.5 eV, which is larger than the value of 3.2eV for bulk TiO<sub>2</sub>. The blue shift might be caused by nanosize effect and structural defect of nanomaterials. Based on the antibacterial studies, the Calcareous/TiO<sub>2</sub> nanocomposites show good accountability on the degradation of growth of pathogens. So the antibacterial properties of TiO<sub>2</sub> nanoparticles are often further explored in future on other bacterial strains, In order that these nanoparticles can be

utilized in various industrial and medical applications.

## CONSENT

It is not applicable.

## ETHICAL APPROVAL

It is not applicable.

## COMPETING INTERESTS

Authors have declared that no competing interests exist.

## REFERENCES

1. Guo-cai XU, Li-de Z. Nanocomposite materials. Beijing: Chemical Industry Press, China; 2002.
2. Cermenati L, Dondi DL, Maurizio F, Angelo A. Titanium dioxide photocatalysis of adamantane. *Tetrahedron*, 2003;59(34):6409-6414.
3. Liu JP, Tian J. Nanotechnology in textile Science. Beijing: China Textile Press, China; 2003.
4. Wu X, Liu H, Liu J, haley KN, Treadway JA, Larson JP, Ge N, Peale F, Bruchez MP. Immunofluorescent labeling of cancer marker Her2 and other cellular targets with semiconductor quantum dots. *Nat Biotechnol* 2003;21(1):41-6.
5. Fortner JD, Lyon DY, Sayes CM, Boyd AM, Falkner JC, Hotze EM, Alemany LB, Tao YJ, Guo W, Ausman KD, Colvin VL, Hughes JB. C-60 in water: Nanocrystal formation and microbial response. *Environ Sci Technol* 2005;39(11):4307-16.
6. Li P, Li J, Wu C, Wu Q, Li J. Synergistic antibacterial effects of lactam antibiotic combined with silver nanoparticles. *Nanotechnol* 2005;16(9):1912-17.
7. Sungkaworn T, Triampo W, nalakarn P, Triampo D, tang IM, Lenbury Y, Picha P. The effects of TiO<sub>2</sub> nanoparticles on tumor cells colonies: fractal dimension and morphological properties. *World Acad Sci Eng Technol, Int J biomed Sci* 2008;2(13):801-08.
8. Herrera M. Carrion P, Baca P, Liebana J, Castillo A. In vitro antibacterial activity of glass-ionomer cements. *Microbios* 2001;104(409):141-48.
9. Pal S, Tak YK, Song JM. Does the antibacterial activity of silver nanoparticles depend on the shape of the nanoparticle? A study of the Gram-negative bacterium, *Escherichia coli*. *Appl Environ Microbiol*. 2007;73(6):1712–1720.
10. Fujishima A, Rao TN, Tryk DA. Titanium dioxide photocatalysis. *J Photochem Photobiol C: Photochem Rev* 2000;1(1):1–21.
11. Amezaga-Madrid P, Nevarez-Moorillon GV, Orrantia-Borunda E, Miki-Yoshida M. Photoinduced bactericidal activity against *Pseudomonas aeruginosa* by TiO<sub>2</sub> based thin film. *FEMS Microbiol Lett* 2002;211(2):183–188.
12. Maness P, Smolinski S, Blake DM, Huang Z, Wolfrum EJ, Jacoby WA. Bactericidal activity of photocatalytic TiO<sub>2</sub> reaction: toward an understanding of its killing mechanism. *Appl Environ Microbiol* 1999;65(9):4094–4098.
13. Stoimenov PK, Klinger RL, Marchin GL, Klabunde KJ. Metal oxide nanoparticles as bactericidal agents. *Langmuir* 2002;18(17):6679–6686.
14. Fresta M, Puglisi G, Giammona G, Cavallaro G, Micali N, Furneri PM. Pefloxacin mesilate loaded and ofloxacin-loaded polyethylcyanoacrylate nanoparticles—characterization of the colloidal drug carrier formulation. *J Pharm Sci* 1995;84(7):895–902.
15. Hamouda T, Hayes M, Cao Z, Tonda R, Johnson K, Craig W, Brisker J, Baker JA novel surfactant nanoemulsion with broad-spectrum sporicidal activity against *Bacillus* species. *J Infect Dis* 1999;180(6):1939–1949.
16. Alivisatos AP. Semiconductor Clusters, Nanocrystals and Quantum Dots. *Science of the Total Environment* 1996;271(5251):933-937.
17. Matsunaga T, Tomoda R, Nakajima T, Wake H. Photoelectrochemical sterilization of microbial cells by semiconductor powders. *FEMS Microbiol. Lett* 1985;29(1-2):211-14.
18. Rincon AG, Pulgarin C. Comparative evaluation of Fe<sup>3+</sup> and TiO<sub>2</sub> photoassisted processes in solar photocatalytic disinfection of water. *Appl. Catal. B: Environ* 2006;63(3-4):222–31.
19. Benabbou AK, Derriche Z, Felix C, Lejeune P, Guillard C. Photocatalytic inactivation of *Escherichia coli*: Effect of concentration of TiO<sub>2</sub> and microorganism, nature, and intensity of UV irradiation. *Appl. Catal. B: Environ* 2007;76(3-4): 257–63.

20. Pigeot-Remy S, Simonet F, Errazuriz-Cerda E, Lazzaroni JC, Atlan D, Guil-lard C. Photocatalysis and disinfection of water: Identification of potential bacterial targets. *Appl. Catal. B: Environ* 2011;104(3-4):390–98.
21. Bindu Arora, Madhura Murar and Vinayak Dhumale, Antimicrobial potential of TiO<sub>2</sub> nanoparticles against MDR *Pseudomonas aeruginosa*, *J. Exp. Nanosci* 2015;10(11):819–827.
22. Lashgari A, Ghamami S, Golzani M, Gram-Negative and Gram- Positive Bacteria; Antibacterial activity of a clay-TiO<sub>2</sub> nanocomposites, *Bulletin of Environment, Pharmacology and Life Sciences, Bull. Env. Pharmacol. Life Sci.* 2016;5(2):53-59.
23. Muhammad AM, Alvin YC, Gil NCS, Structures, Morphological Control, and Antibacterial Performance of Ag/TiO<sub>2</sub> Micro-Nanocomposite Materials, *Adv. Mater. Sci. Eng* 2019;1-12.
24. Sahar EA, Hussein AM, Emad ME, Antimicrobial activity of functionalised carbon nanotubes against pathogenic microorganisms, *IET Nanobiotechnol.*, 2020;14(6):457-64
25. Popov AP, Dimitrieva AI, Kovalenko AV, Yumanov DS, Stepanov AV, Shemukhin AA, Vorobyeva EA, Emad ME, The structure of multi-walled carbon nanotubes as a factor affecting the life of *E. Coli*, *J. Phys. Conf. Ser.* 2020;1611:1-6.
26. Matei E, Enculescu I, Enculescu M, Neumann R, Enculescu I. Effect of additives on nickel nano wires electrochemical deposition. *J. Optoelectron. Adv. M.* 2008;10(3):508-11.
27. Zakeri SME, Asghari M, Feilizadeh M, M. Vosoughi M. A visible light driven doped TiO<sub>2</sub> nanophotocatalyst: Preparation and characterization. *Int. J. Nano Dimens* 2014;5(4):329-35.
28. Kalayani G, Anil VG, Bo-Jung C, Yong-Chien L. Preparation and characterization of ZnO nanoparticles coated paper and its antibacterial activity study. *J. Green chem.* 2006;8:1034-41.
29. Mehrizad A, Gharbani P. Study on Catalytic and Photocatalytic Decontamination of (2-Chloroethyl) Phenyl Sulfide with Nano-TiO<sub>2</sub>. *Int. J. Nanosci. Nanotechnol* 2011;7(1):48-53.
30. Noroozifar M, Khorasani-Motlagh M, and Z. Yavari Z. Effect of Nano-TiO<sub>2</sub> Particles on the Corrosion Behavior of Chromium-Based Coatings. *Int. J. Nanosci. Nanotechnol* 2013;9(2):85-94.
31. Mariselvi P, Anantha kumar T, Veeraputhiran V, Alagumuthu G. Synthesis, Characterization and Photocatalytic Activity of Calcareous/TiO<sub>2</sub> Nanocomposites under UV Light Irradiation using Methylene Blue Dye. *J. Nanosci. Tech* 2019;5(1):599–602.
32. Haque FS, Sen KS, Pal CS. Nutrient optimization for production of broad spectrum antibiotics by *Streptomyces*, *Antibiotics Str.* 15.4. *Acta Microbiol. Immunol. Hung* 1995; 42(2): 155-62.
33. Chen D, Zhu Q, Zhou F, Deng X, Li, F. Synthesis and photocatalytic performances of the TiO<sub>2</sub> pillared montmorillonite. *J. Hazard. Mater* 2012;235-236:186-93.
34. Sagadevan S. Synthesis and electrical properties of TiO<sub>2</sub> nanoparticles using a wet chemical techniques. *Am J Nanosci & Tech* 2013;1(1):27-30.
35. Rajakumar G, Rahuman AA, Priyamvada B, Khanna VG, Kumar DK, Sujin PJ. *Eclipta prostrata* leaf aqueous extract mediated synthesis of titanium dioxide nanoparticles. *Mater. Lett* 2012;68:115–17
36. Oganisian K, Hreniak A, Sikora A, Gaworska-Koniarek D, Iwan A. Synthesis of iron doped titanium dioxide by sol-gel method for magnetic applications. *Process and Appl. of Cera* 2015;9(1): 43–51.
37. Nabiyounil G, Sahraei R, Toghiany M, Majles M, Hedayati K. Preparation and Characterization of Nano-Structured ZnS thin films Grown on Glass and N-type Si Substrates using a New Chemical Bath Deposition Technique. *Rev. Adv. Mater. Sci* 2011;27: 52-57.
38. Zulkiflee NS, Hussin R, Halim J, Ibrahim MI, Zainal MZ, Nizam S, Rahman SA. Characterization of TiO<sub>2</sub>, ZnO, and TiO<sub>2</sub>/ZnO thin films prepared by sol-gel method. *ARPJ. J. Eng. Appl. Sci* 2016;11(12):7633-37.
39. Saja S, Taweel A, Saud HR. New route for synthesis of pure anatase TiO<sub>2</sub> nanoparticles via ultrasound assisted sol-gel method. *J. chem. pharm. res* 2016;8(2):620-26.
40. Tayebi N, Andreas AP. Modeling the effect of skewness and kurtosis on the static friction coefficient of rough surfaces. *Tribol Int.* 2004;37(6):491-505.
41. Quinones-Juradol ZV, Waldo-Mendoza MA, Aguilera-Bandin HM, Villabona-Leal

- EG, Cervantes-Gonzalez E, Perez E. Silver Nanoparticles Supported on TiO<sub>2</sub> and Their Antibacterial Properties: Effect of Surface Confinement and Nonexistence of Plasmon Resonance. *Mater Sci and Appl.* 2014;5(12):895-903.
42. Jayaseelan C, Rahuman AA, Roopan SM, Kirthi AV, Venkatesan J, Kim S, Iyappan M, Siva C. Biological approach to synthesize TiO<sub>2</sub> nanoparticles using *Aeromonas hydrophila* and its antibacterial activity. *Spectrochim. Acta A Mol. Biomol.* 2013;107:82–89.
43. Koseki H, Shiraishi K, Asahara T, Tsurumoto T, Shindo H, Baba K, Taoda, H Terasaki, N. Photocatalytic bactericidal action of fluorescent light in a titanium dioxide particle mixture: an in vitro study. *Biomed. Res* 2009; 30(3): 189-92.
44. Mariselvi P, Alagumuthu G, Synthesis, characterization and antibacterial activity of illite/TiO<sub>2</sub> Nanocomposites, *Int. j. appl. Res.* 2016;2(4):553-556.
45. Mariselvi P, Alagumuthu G, Structural, Morphological and Antibacterial Activity of Kaolinite/TiO<sub>2</sub> Nanocomposites, *J. Nanosci. Tech.* 2015; 1(1):16–18.
46. Pohan LAG, Kambire O, Nasir M, Ouattara L. Photocatalytic and Antimicrobial Properties of [AgTiO<sub>2</sub>]:[Clay] Nanocomposite Prepared with Clay Different Ratios, *Mod. Res. Cata.* 2020;9:47-61.
47. Ragupathy S and Raghu K. Studies on preparation of TiO<sub>2</sub> Nanoparticles and its loaded groundnut shell activated carbon and their antibacterial activity, *Int. J. Adv. Res. Biol. Sci.* 2014;1(9):08–13.
48. Alireza A, Jalali SAH, Hamid B, Hossein A. Preparation, characterization, and antibacterial activity of NiFe<sub>2</sub>O<sub>4</sub>/PAMA/Ag–TiO<sub>2</sub> nanocomposite, *J. Magn. Magn. Mater* 2016;40:14-20.

© 2021 Mariselvi and Kumar; This is an Open Access article distributed under the terms of the Creative Commons Attribution License (<http://creativecommons.org/licenses/by/4.0>), which permits unrestricted use, distribution, and reproduction in any medium, provided the original work is properly cited.

*Peer-review history:*

*The peer review history for this paper can be accessed here:*  
<https://www.sdiarticle4.com/review-history/72834>